Infection, Genetics and Evolution 11 (2011) 987–996

Contents lists available at ScienceDirect

Infection, Genetics and Evolution

journal homepage: www.elsevier.com/locate/meegid

Characterization of California sea lion polyomavirus 1: Expansion of the known host range of the Polyomaviridae to Carnivora

James F.X. Wellehan Jr.[a,*], Rebecca Rivera[b], Linda L. Archer[a], Celeste Benham[b], Jennifer K. Muller[a], Kathleen M. Colegrove[c], Frances M.D. Gulland[d], Judy A. St. Leger[e], Stephanie K. Venn-Watson[f], Hendrik H. Nollens[a,b,c]

[a] Marine Animal Disease Laboratory, College of Veterinary Medicine, University of Florida, Gainesville, FL 32610, USA
[b] Hubbs-SeaWorld Research Institute, San Diego, CA 92109, USA
[c] University of Illinois Zoological Pathology Program, Loyola University Medical Center, Building 101, Room 0745, 2160 South First Avenue, Maywood, IL 60153, USA
[d] The Marine Mammal Center, Fort Cronkhite, CA 94965, USA
[e] SeaWorld, San Diego, 500 SeaWorld Drive, San Diego, CA 92109, USA
[f] Navy Marine Mammal Program Foundation, 1220 Rosecrans St, San Diego, CA 92106, USA

ARTICLE INFO

Article history:
Received 6 September 2010
Received in revised form 11 February 2011
Accepted 17 March 2011
Available online 29 March 2011

Keywords:
California sea lion
Phylogeny
Polyomaviridae
Quantitiative PCR
Rolling circle amplification
Zalophus californianus

ABSTRACT

The genome of a novel polyomavirus first identified in a proliferative tongue lesion of a California sea lion (*Zalophus californianus*) is reported. This is only the third described polyomavirus of laurasiatherian mammals, is the first of the three associated with a lesion, and is the first known polyomavirus of a host in the order Carnivora. Predicted large T, small t, VP1, VP2, and VP3 genes were identified based on homology to proteins of known polyomaviruses, and a putative agnoprotein was identified based upon its location in the genome. Phylogenetic analysis of the predicted late region proteins found that the laurasiatherian polyomaviruses, together with Squirrel monkey polyomavirus and Murine pneumotropic virus, form a monophyletic clade. Phylogenetic analysis of the early region was more ambiguous. The noncoding control region of California sea lion polyomavirus 1 is unusual in that only two apparent large T binding sites are present; this is less than any other known polyomavirus. The VP1 of this virus has an unusually long carboxy-terminal region. A quantitative polymerase chain reaction was developed and utilized on various samples from 79 additional animals from either managed or wild stranded California sea lion populations, and California sea lion polyomavirus 1 infection was found in 24% of stranded animals. Sequence of additional samples identified four sites of variation in the t antigens, three of which resulted in predicted coding changes.

1. Introduction

Polyomaviruses (PyV) are nonenveloped circular DNA viruses with bidirectional transcription from a non-coding control region (NCCR). The early region encodes overlapping nonstructural proteins, consisting of a large T antigen, a small t antigen, and in some species also a middle T antigen, which initiate viral replication and promote cell cycle progression. The late region, in the opposite direction, encodes capsid proteins VP1 and VP2/VP3 (Imperiale and Major, 2007). In some species, an agnoprotein (called VP4 in avian polyomaviruses) is also encoded in the 5′ late region. Agnoproteins are usually highly basic proteins that are involved in capsid assembly, cell cycle dysregulation, induction of apoptosis, and inhibition of DNA repair (Khalili et al., 2005; Johne et al., 2007). The agnoprotein is generally the least conserved polyomavirus protein, and there is little homology between agnoproteins of more divergent polyomaviruses (Verschoor et al., 2008). The NCCR controls transcription and also contains the origin of replication. The NCCR is defined as the region between the T-antigen start codon in the early region and the agnoprotein start codon in the late region (White et al., 2009). In species without an agnoprotein, the VP2 start codon is the end point of the NCCR. Rearrangement may occur within the NCCR and may alter clinical significance (Sroller et al., 2008).

Mammalian PyVs are thought to have a narrow host range (Imperiale and Major, 2007). However, evidence suggests that JC virus, a human PyV, has had a very rapid radiation in humans, and it has been proposed that this may be due to a recent host switch into humans from another species (Mes et al., 2010). The best-studied

Abbreviations: PyV, Polyomavirus; NCCR, non-coding control region.

* Corresponding author. Tel.: +1 352 392 2226; fax: +1 352 392 4877.
E-mail address: wellehanj@ufl.edu (James F.X. Wellehan Jr.).

1567-1348/$ – see front matter © 2011 Elsevier B.V. All rights reserved.
doi:10.1016/j.meegid.2011.03.010

avian PyV, Budgerigar PyV, has a fairly broad host range in which productive infections may be seen in a variety of species (Arroube et al., 2009).

Polyomaviruses most commonly cause life-long subclinical infection in endemic immunocompetent hosts. However, they may cause fatal disease in immunocompromised animals (Jiang et al., 2009). There is precedent for polyomaviral pathogenesis in healthy animals; Budgerigar PyV can cause fatal hepatitis, ascites, and hydropericardium in apparently healthy parrot fledglings, and goose hemorrhagic polyomavirus can cause hemorrhagic nephritis and enteritis in apparently healthy goslings (Johne and Müller, 2007). Merkel cell polyomavirus has been strongly associated with the majority of Merkel cell carcinomas in humans (Sastre-Garau et al., 2009). Most importantly from a host/virus relationship standpoint, they can cause tumor formation when non-productive infection occurs in an aberrant host (Dougherty, 1976; Giardi et al., 1962; London et al., 1978, 1983; Walker et al., 1973). Host phylogenetic distances play significant roles in the ability of viruses to infect aberrant hosts (Pinkerton et al., 2008; Streicker et al., 2010).

The longer-term evolutionary relationships of the polyomaviruses and their hosts are poorly understood, and there is a large taxonomic bias in the known host range of the Polyomaviridae. Placental mammals are divided into four main superorders: two less speciose clades, Afrotheria (including elephants, aardvarks, and others) and Xenarthra (armadillos/sloths/anteaters), and two larger clades containing most mammal species, Laurasiatheria (containing the species of greatest veterinary significance, including horses, cattle, and the order Carnivora, which includes dogs and cats) and Euarchontoglires (primates/rabbits/rodents) (Murphy et al., 2001). Most known mammalian PyV are from Euarchontoglire hosts. The best investigated host species, *Homo sapiens*, has eight known endemic polyomaviruses. Only two PyVs are recognized from laurasiatherian hosts; one from cows (*Bos taurus*) and one from two closely related bat species (*Myotis lucifugus* and *M. californicus*) (Misra et al., 2009). Evidence supporting the presence of natural PyV infection in the order Carnivora has not been previously reported. An immunohistologic survey of formalin-fixed vaccine-associated sarcomas from domestic cats found no evidence of murine polyomavirus antigen, and PCR screening using Bovine PyV primers and consensus PyV primers resulted in no amplification (Kidney et al., 2001).

With aberrant host infections as a significant concern with PyV infections, a greater understanding of PyV diversity and host relationships is needed. This report describes the genome of the first PyV from a host in the Carnivora, phylogenetic analysis of this virus, development of a quantitative PCR (qPCR) for detection of this virus, and use of this qPCR to survey tissues from wild and managed sea lion populations for the virus.

2. Materials and methods

2.1. Samples

Index case: An adult female California sea lion (*Zalophus californianus*) was found stranded along the central California

Table 1
qPCR results for CSLPyV1. Numbers represent copy numbers detected. Wild stranded animals are not bolded, and animals from a managed collection housed in open bay net pens are in bold. Samples from formalin-fixed paraffin-embedded tissues are marked as FFPE; all others are frozen samples.

Tissue	Copies detected	Animal ID number	*n*
Kidney	0	1 (FFPE), 2–5, 7–9, 11–13, 15–18, 21–23, 25, 27, 29, 33, 36–43, 50–53, **55**	35 of 45
	3	34	1 of 45
	11	32	1 of 45
	14	19	1 of 45
	15	44	1 of 45
	21	6	1 of 45
	22	20	1 of 45
	56	45	1 of 45
	58	14	1 of 45
	102	28	1 of 45
	15083	10	1 of 45
Urine	0	2–5, 7–23, 30–31, 33–41, 44, 46–47, **56**	36 of 38
	26	1	1 of 38
	40	6	1 of 38
Urinary bladder	0	1, 50–52, **55**	5 of 5
Cervix	4	1	1 of 1
Vagina	0	54	1 of 3
	8	1 (proximal)	1 of 3
	17	1 (tumor)	1 of 3
Muscle	0	23	1 of 1
Pericardial fluid	0	**55**	1 of 1
Lung	0	50–53	4 of 4
Trachea	0	50–52	3 of 3
Buffy coat	0	**55–80**	26 of 26
Lymph node	0	49–52, **55**	5 of 6
	74	1 (FFPE)	1 of 6
Spleen	0	50–54, **55**	6 of 6
Brain	0	23, 50–52	4 of 4
Skin	0	48, 50–54	6 of 6
Mammary	0	54	1 of 1
Tongue	0	21–22, 25–27	5 of 6
	310	24	1 of 6
Oral mucosa	0	26	1 of 1
Esophagus	0	54, **55**	2 of 3
	78	1	1 of 3
Intestine	0	1 (FFPE)	1 of 1
Liver	0	23, 50–53, **55**	6 of 7
	1415	1	1 of 7
Mediastinum	7	49	1 of 1

coast with a mass on the tongue containing intranuclear inclusions, which were found by electron microscopy to have virions consistent with Polyomaviridae. Full pathologic description is available elsewhere (Colegrove et al., 2010). Tissues examined by qPCR included frozen liver, esophagus, cervix, proximal vagina, vaginal tumor, urine, and urinary bladder, and formalin-fixed paraffin-embedded lymph node, intestine with lymphoma, and kidney.

Additional animals: Various samples from 53 additional stranded wild sea lions from California and 26 animals from a managed collection housed in open bay net pens were examined by quantitative PCR (qPCR) (see Table 1).

2.2. Amplification and sequencing, and gene identification

DNA was extracted from the tongue lesion tissue using a DNeasy Kit (Qiagen, Valencia, CA). Rolling circle amplification was performed with a commercial kit (TempliPhi DNA, Amersham Biosciences, Piscataway, NJ) following the manufacturer's instructions. Products were digested using EcoRI enzyme (Invitrogen, Carlsbad, CA), cloned into pUC18 (Clontech, Mountain View, CA), expanded in One Shot Max Efficiency DH5alpha-T1R Competent Cells (Invitrogen) and sequenced using M13 primers.

To complete the genome, two nested PCRs were designed. The first nested PCR used primers T-103F1 and VP1-136R1 in the first round, and primers T-25F2 and VP1-70R2 in the second round (Table 2). The second nested PCR used primers VP1-778F1 and T-84R1 in the first round and VP1-868F2 and T_105R2 in the second round. Amplifications were performed using Takara SpeedStar HS DNA Polymerase (Takara Bio Inc, Otsu, Japan) as follows: 1 min denaturation at 94 °C, followed by 35 cycles of denaturation at 95 °C (5 s), annealing at 58 °C (15 s), extension at 72 °C (30 s), with a final elongation step at 72 °C for 5 min. PCR products were run in agarose gels and bands were cut and extracted using the Qiaquick gel extraction kit (Qiagen, Valencia, CA). Direct sequencing was performed using the Big-Dye Terminator Kit (Applied Biosystems, Foster City, CA) and ABI automated sequencers. Additional primers were used for primer walking to complete the sequence (see Table 2). All sequence had at least two-fold coverage in both directions, and primer sequences were edited out prior to constructing contiguous sequences.

Table 2
Primers used in this study.

Primer ID	Primer sequence 5′–3′	Use
T-103F1	GCATTTCCCCACATATCCTC	Nested PCR to close gaps
VP1-136R1	GGTGTCTCTGTCCCACCTGT	
T-25F2	TTGCATTTGTCCTCATCACC	
VP1-70R2	TGCCAGCATTCAACAGGATA	
VP1-778F1	GACATAGAAGCCCCAGACCA	
T-84R1	GAGGATATGTGGGGAAATGC	
VP1-868F2	AGGATTCAGATGACGCAACC	
T_105R2	GGGCCTTCCTGGAGATCTAA	
T21-529R	TCCCCCTGGTATTGTCACAT	Sequencing primers for primer walking
T21-512F	GTGACAATACCAGGGGGAAA	
T22-596F	GGTGTGCTGTCCTGGGTATT	
T22-615R	AATACCCAGGACAGCACACC	
CSLPyV-281R	GACAGGGCCTTGAACAGAAA	
CSLPyV-909R	TTGCAGCTTCTCCCAAAGAT	
CSLPyV-760F	TGGACGAGGTTGCTTATGTG	
CSLPyV-1606F	CAGGTGCCAAAACTCCTCAT	
CSLPyV-1727R	TCATGCTCTGTTGGTGTTCC	
PyV-F	CCACCACCGCCTGCTAGT	Quantitative PCR
PyV-R	GGTCCTCTTGCATGTCCAGATAA	
PyV-probe	6FAM-CTCAACCCCCTCCTAT-MGBNFQ	
VP1-603F2	AGAGGTCCCTTGGAGGTTGT	Heminested PCR
VP1-797R1	TGGTCTGGGGCTTCTATGTC	
VP1-765R2	CTACCCTGTTTTCCCCTTCC	

Open reading frames (ORFs) were identified using a web-based translator (http://www.vivo.colostate.edu/molkit/translate/index.html). Large ORFs were identified by sequence homology to known polyomaviruses in GenBank (National Center for Biotechnology Information, Bethesda, MD), EMBL (Cambridge, United Kingdom), and Data Bank of Japan (Mishima, Shizuoka, Japan) databases using BLASTP (Altschul et al., 1997).

2.3. Examination of the NCCR from additional samples

To look for variation, the NCCR and partial flanking regions were amplified from three samples in addition to the original tongue lesion; liver from the index case (animal 1), kidney from animal 10, and tongue from animal 24 (see Table 1). DNA samples were amplified and sequenced with primers T-103F1 and CSLPyV-909R (Table 2) using conditions described above for gap closing.

2.4. Large T splicing site

To determine the sequence of the mature Large T antigen mRNA, RNA was extracted from kidney from animal 10 and tongue from animal 24 (see Table 1) using the RNeasy Mini Kit (Qiagen). Reverse transcription PCR was performed using the OneStep RT-PCR Kit (Qiagen) according to standard protocol using primers T22-596F and T-84R1 (Table 2). There was a reverse transcription at 50 °C for 30 min, followed by a denaturation at 94 °C for 5 min, then 36 cycles of denaturation at 94 °C for 30 s; annealing at 58 °C for 30 s, DNA extension at 72 °C for 45 s, and a final extension step at 72 °C for 10 min. Two μl of product from the first reaction was used in a second round of PCR amplification with primers T22-596F and T-105R2. The mixtures were amplified in a thermal cycler (PCR Sprint, Thermo Hybaid) with an initial denaturation at 94 °C for 5 min, followed by 36 cycles of denaturation at 94 °C for 45 s; annealing at 58 °C for 45 s, DNA extension at 72 °C for 90 s, and a final extension step at 72 °C for 10 min. The PCR products were resolved in 1% agarose gels, and excised, purified, and sequenced as above. All products were sequenced in both directions.

2.5. Phylogenetic analysis

The predicted homologous amino acid sequences of polyomaviral proteins were aligned using MAFFT (Katoh and Toh, 2008). Since the Large T protein shares one of its two exons with the small t, the large T analysis considers only the unique second exon. Bayesian analyses of each alignment were performed using MrBayes 3.1 (Ronquist and Huelsenbeck, 2003) with gamma distributed rate variation and a proportion of invariant sites, and amino acid substitution model jumping. Four chains were run and statistical convergence was assessed by looking at the standard deviation of split frequencies as well as potential scale reduction factors of parameters. The first 10% of 1,000,000 iterations were discarded as a burn in, based on examination of trends of the log probability vs. generation. Two independent Bayesian analyses were run to avoid entrapment on local optima.

Maximum likelihood (ML) analyses of each alignment were performed using PHYLIP (Phylogeny Inference Package, Version 3.66) (Felsenstein, 1989), running each alignment using the program Proml with amino acid substitution models JTT (Jones et al., 1992), PMB (Veerassamy et al., 2003), and PAM (Kosiol and Goldman, 2005) further set with global rearrangements, five replications of random input order, gamma plus invariant rate distributions, and unrooted. The values for the gamma distribution were taken from the Bayesian analysis. Bandicoot papillomatosis carcinomatosis virus 1 (Bandicoot PCV1, GenBank accession number NC010107) was used as the outgroup for the early genes, and Goose polyomavirus (AY140894) was designated as the

outgroup for the late genes. The alignment was then used to create data subsets for bootstrap analysis to test the strength of the tree topology (1000 re-samplings) (Felsenstein, 1985), which was analyzed using the amino acid substitution model producing the most likely tree in that alignment. Recombination analysis using multiple methods in the RDP3 suite was performed (Martin et al., 2005).

2.6. Quantitative PCR

Quantitative PCR was performed using forward primer PyV-F, reverse primer PyV-R, and probe PyV-probe targeting the California sea lion polyomavirus 1 (CSLPyV1) VP1 gene (Table 2). Each 20 μL reaction was run in duplicate, and was 0.9 μM for each primer and 0.25 μM for the probe, and contained 7 μl of extracted DNA and 10 μl of a commercial universal qPCR mix (TaqMan® Fast Universal PCR Master Mix 2X, Applied Biosystems), using a standard fast protocol. A Eukaryotic 18S rRNA Endogenous Control primer/probe set (Applied Biosystems) was used as a control for each sample in a separate well. The standard curve, run on each plate, used a 10-fold serial dilution of a CSLPyV1 PCR amplicon from the index case, ranging from 10^6 to 10 copies. A 7500 Fast Real-Time PCR System (Applied Biosystems) was used to amplify the reactions with cycling conditions as follows: initial denaturation at 95 °C for 20 s; 50 cycles of 95 °C for 3 s followed by 60 °C for 30 s. Samples with an appropriate curve but a Ct consistent with less than 25 copies were confirmed using heminested PCR and sequencing of PCR products. This confirmatory PCR used forward primer VP1-603F2 and VP1-797R1 as a first round, and VP1-603F2 and VP1-765R2 as a second round (Table 2). Amplifications were performed using Platinum Taq DNA polymerase (Invitrogen) as follows: 5 min denaturation at 94 °C, followed by 36 cycles of denaturation at 95 °C (45 s), annealing at 58 °C (45 s), extension at 72 °C (30 s), with a final elongation step at 72 °C for 10 min. Products were electrophoresed and sequenced as above. Results from the qPCR that were not confirmed by the heminested PCR were considered negative.

3. Results

3.1. Amplification, sequencing, and gene identification

The complete circular genome obtained was 5112 base pairs. The sequence was submitted to GenBank under accession number GQ331138. The virus is hereafter referred to as California sea lion polyomavirus 1 (CSLPyV1). VP1, VP2, VP3, small t, and large T proteins were identified on the basis of homology to known polyomaviral proteins (Fig. 1). The VP1 protein had a carboxy-terminal portion that extended 135 amino acids beyond homologous VP1 proteins. A possible agnoprotein was identified on the basis of location in the genome, although no significant homology to known agnoproteins was identified using BLASTP. This predicted agnoprotein was found to be very basic, with a predicted isoelectric point of 10.6 using pepstats (http://www.ebi.ac.uk/Tools/emboss/pepinfo/), consistent with other polyomaviral agnoproteins. The NCCR of CSLPyV1 contained only two predicted large T binding sites (GRGGC) in opposite orientations in a nearly palindromic region (Fig. 2). Even when the possibility that the predicted agnoprotein was actually nocoding sequence was considered, and the analysis was extended to the predicted VP2 start codon, only two additional large T binding sites were detected, and they were not clustered together (Fig. 2). The 5′ end of the NCCR had an 18 base pair region of high homology with Squirrel Monkey PyV (SqMPyV) and Myotis PyV, differing by one nucleotide and by two nucleotides and an indel, respectively (Fig. 2).

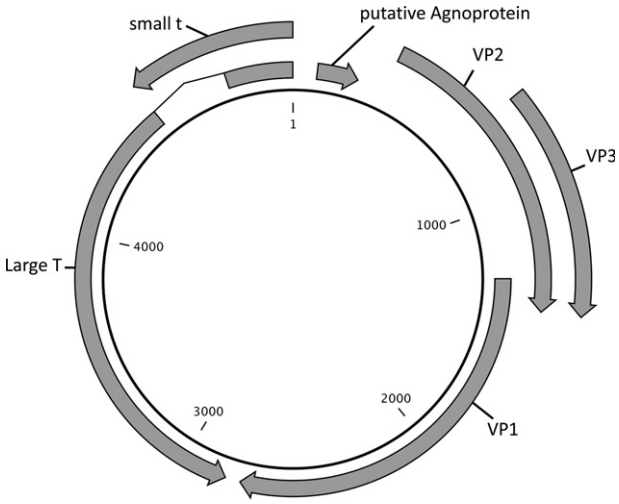

Fig. 1. Genome organization of CSLPyV1.

3.2. Examination of the NCCR from additional samples

Alterations in the NCCR have been associated with disease (White et al., 2009), and it was plausible that the NCCR sequence

```
1    CTTTTTTGCAGGTGCTGAAAGCCTGAAGGGCCAGCTGCTGCTTCTCCAACTTAAGGAAAT
SqM  CTTTTTTTCAGGTGCTGA
Myo  CTTTTTT-CAGGTGGTGG

61   AAGGTAGGTGGCAAAAAAAGCCTCTGGGGCTTTATATGAAAAAAATTCTGAGGTTGGCTC

121  TTTGCCCAGACGGTGTCCGGTTACCGGCTTGCCCCGGATTTGCTTACTGGGCCGTCGCTC

181  CTCCCAGTGCCGGCCCATTTGGCCCTCAGCCACTGTTATTGCTCACACGTGGCGCACAGC

241  CAAAGTGAAACTAAAGTGGAAGCTGGCCAATAACGGCCTCTGGGCCGCTGCCAGCTTCCC

301  GCTTTGGCCTACTTTTTTGCCTCTAGAAGCCTGCTCTAAGGTAAGATTTCTTATTTTCTA

361  GGT
```

Fig. 2. The noncoding control region and putative agnoprotein coding region of CSLPyV1. The underlined region has high homology with Squirrel Monkey PyV (SqM) and Myotis PyV (Myo). Differences are shaded dark grey. Large T antigen binding sites (GRGGC) are boxed. A near-palindromic region representing a probable origin of replication is shaded light grey. The putative agnoprotein coding region is in bold.

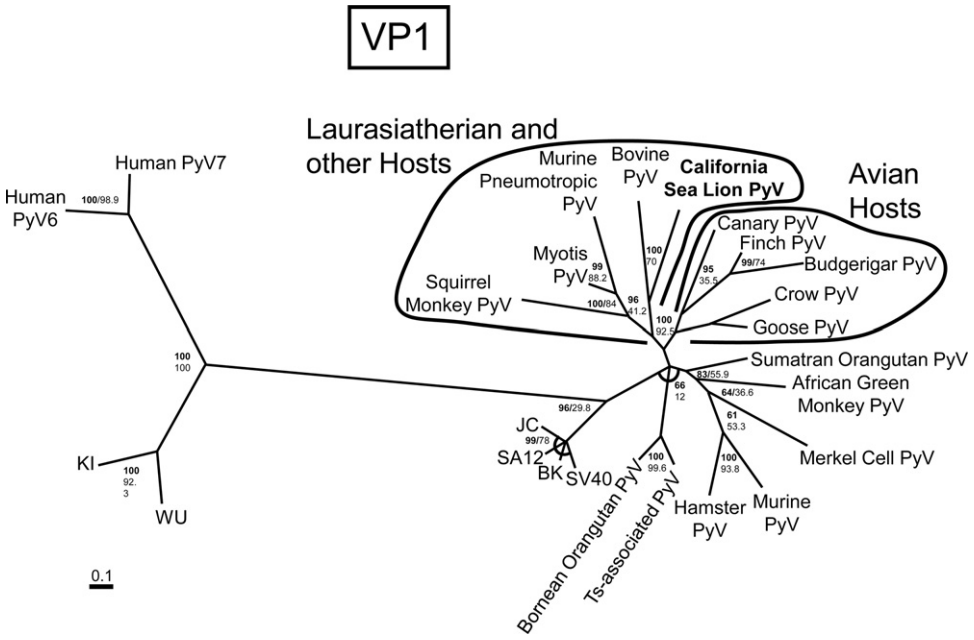

Fig. 3. Bayesian phylogenetic tree of predicted 343–495 amino acid polyomaviral VP1 sequences based on MAFFT alignment. Bayesian posterior probabilities of clusters as percentages are in bold, and ML bootstrap values for clusters based on 200 re-samplings are given to the right. Goose polyomavirus (GenBank accession number AY140894) was designated as the outgroup. California sea lion polyomavirus 1 is bolded. Brackets show clades with avian PyV and laurasiatherian/squirrel monkey/murine pneumotropic PyVs. Sequences retrieved from GenBank include Merkel cell polyomavirus (GenBank accession # EU375803), WU virus 3 (EF444549), KI virus (EF127906), Squirrel monkey polyomavirus (AM748741), Myotis polyomavirus (FJ188392), Crow polyomavirus (DQ192570), Finch polyomavirus (DQ192571), SV40 (J02400), Murine polyomavirus strain A3 (J02289), JC virus (J02226), Budgerigar polyomavirus (AF241168), Bovine polyomavirus (D13942), BK virus (V01108), African green monkey polyomavirus (K02562), Hamster polyomavirus (X02449), SA12 (NC_007611), Murine Pneumotropic virus (NC001505), Trichodysplasia spinulosa-associated polyomavirus (NC014361), Human polyomavirus 6 (NC014406), Human polyomavirus 7 (NC014407), Bornean orangutan polyomavirus (NC013439), Sumatran orangutan polyomavirus (FN356901), and Canary polyomavirus (GU345044).

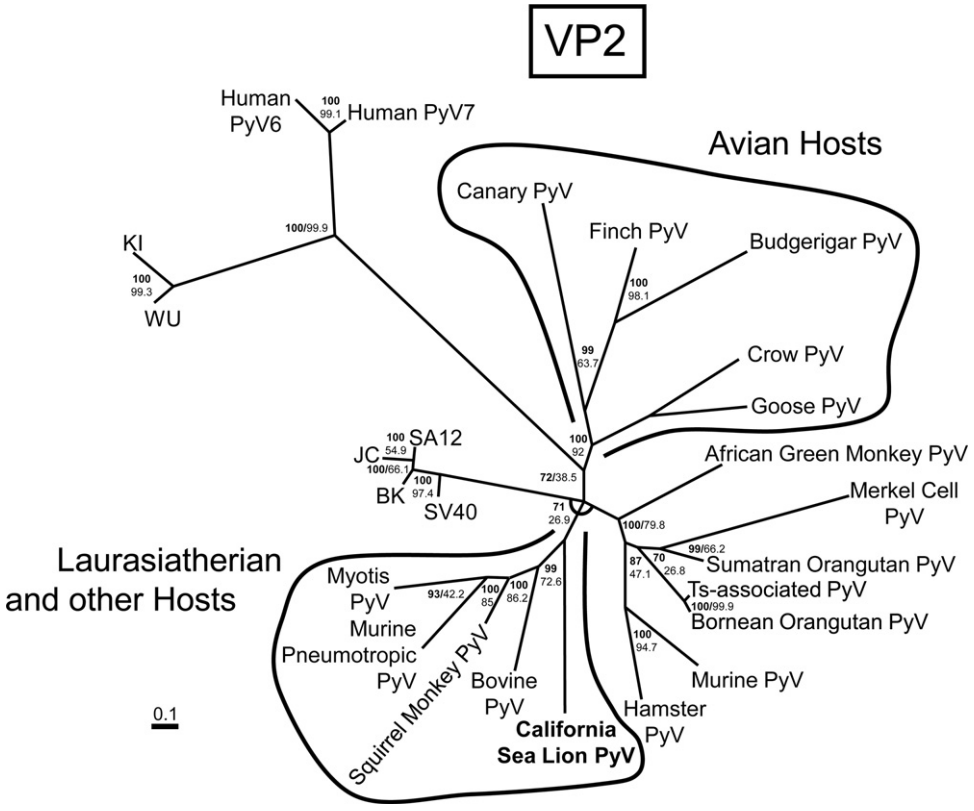

Fig. 4. Bayesian phylogenetic tree of predicted 241–415 amino acid polyomaviral VP2 sequences based on MAFFT alignment. Bayesian posterior probabilities of clusters as percentages are in bold, and ML bootstrap values for clusters based on 200 re-samplings are given to the right. Goose polyomavirus (GenBank accession number AY140894) was designated as the outgroup. California sea lion polyomavirus 1 is bolded. Brackets show clades with avian PyV and laurasiatherian/squirrel monkey/murine pneumotropic PyVs. Sequences retrieved from GenBank are as given in the legend for Fig. 2.

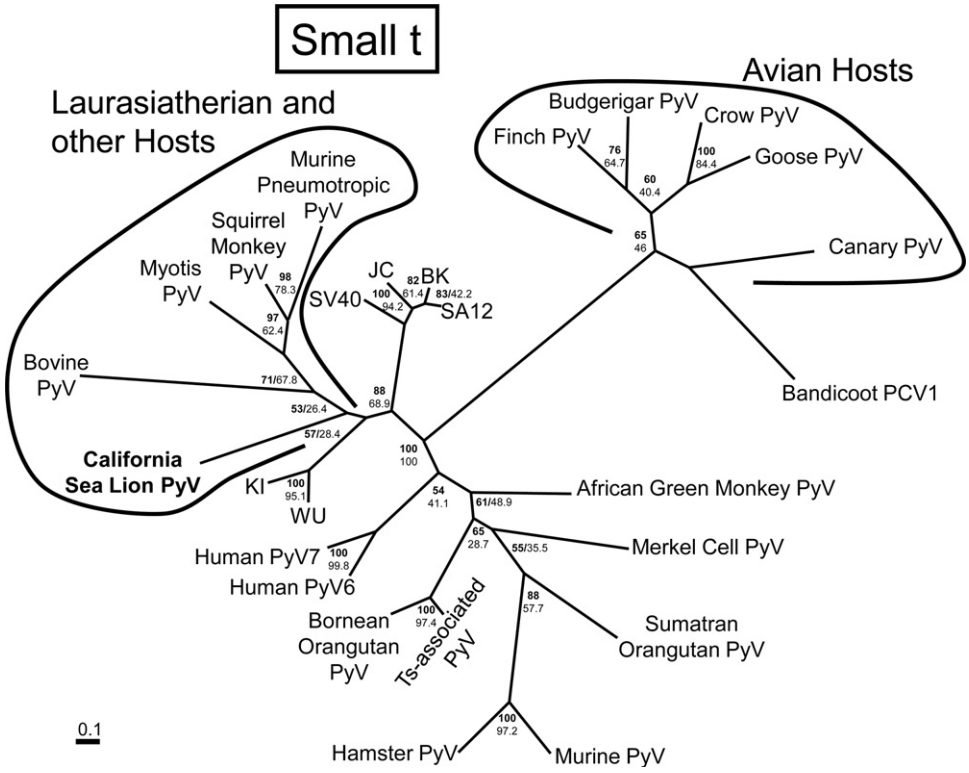

Fig. 5. Bayesian phylogenetic tree of predicted 124–224 amino acid polyomaviral small t sequences based on MAFFT alignment. Bayesian posterior probabilities of clusters as percentages are in bold, and ML bootstrap values for clusters based on 200 re-samplings are given to the right. Bandicoot papillomatosis carcinomatosis virus 1 (GenBank accession number NC010107) was designated as the outgroup. California sea lion polyomavirus 1 is bolded. Bracket shows avian PyV clade and poorly supported laurasiatherian/squirrel monkey/murine pneumotropic clade. Sequences retrieved from GenBank are as given in the legend for Fig. 2.

could have been altered in the initial lesion. PCR and sequencing of all three additional samples resulted in 821 bp of sequence after primers were edited out. Sequence from the liver sample from case 1 was identical to that from the tongue sample, indicating that this is the typical NCCR for CSLPyV1 and pathology was not due to NCCR mutation. Sequence of amplicons from both the kidney from animal 10 and the tongue from animal 24 showed a C to G transversion at position 5077 and a T to C transition at position 5096. These changes resulted in an Asn to Ser change at amino acid 6 and a Glu to Asp change at amino acid 12 of the predicted T antigens. No variation was found in the predicted NCCR region, the putative agnoprotein, or the 3′ section of the VP2 gene. Sequences were submitted to GenBank under accession numbers HM130529–31.

3.3. Large T splicing site

Amplification of both samples resulted in a 458 bp product. A 158 bp product was also seen from the kidney from animal 10. Sequence of the 458 bp products showed that the larger products were consistent with the previously sequenced genome; the product from the tongue of animal 24 was identical to the index sequence. The 458 bp product from kidney from animal 10 the differed by two nucleotides; a C to T transition at position 4744 and a T to G transversion at position 4549. The transition did not result in a coding change but the transversion resulted in a Glu to Asp at position 99 of the predicted small T antigen.

Sequence of the 158 bp cDNA product showed that a 300 bp segment corresponding to nucleotides 4552–4851 had been spliced out, homologous to the intron of the large T antigen of other polyomaviruses. Sequences were submitted to GenBank under accession numbers HM130532 through HM130534.

3.4. Phylogenetic analysis

Bayesian phylogenetic analysis of the VP1 protein found that the rtREV model of amino acid substitution was most probable with a posterior probability of 1.000 (Dimmic et al., 2002). The VP2 analysis found the WAG model to be most probable (posterior probability = 1.000), the Large T analysis found the rtREV model to be most probable, (posterior probability = 1.000), and the small t analysis found the Blosum model to be most probable (posterior probability = 1.000) (Henikoff and Henikoff, 1992; Whelan and Goldman, 2001). Bayesian trees including posterior probabilities of clades are shown (Figs. 3–6).

ML analyses of the VP1 protein found the most likely tree resulted from the JTT model of amino acid substitution, and analysis of the VP2, small t and large T proteins found that the most likely tree resulted from the PMB model. These parameters were used for bootstrap analysis. Bootstrap values from ML analysis are shown on the Bayesian trees (Figs. 3–6).

Genes in the late region showed that the laurasiatherian PyVs together with SqMPyV and Murine Pneumotropic virus (MPtV) form a monophyletic clade. This was not supported in the early region, where the support levels for clusters generally tended to be lower.

Recombination analysis using multiple methods in the RDP3 suite did not reveal evidence of recombination between the early and late regions of CSLPyV1 and other polyomavirus species (data not shown).

3.5. Quantitative PCR

From the index case, frozen liver had the highest virus load with 1415 copies detected in the sample by qPCR. Frozen esophagus also

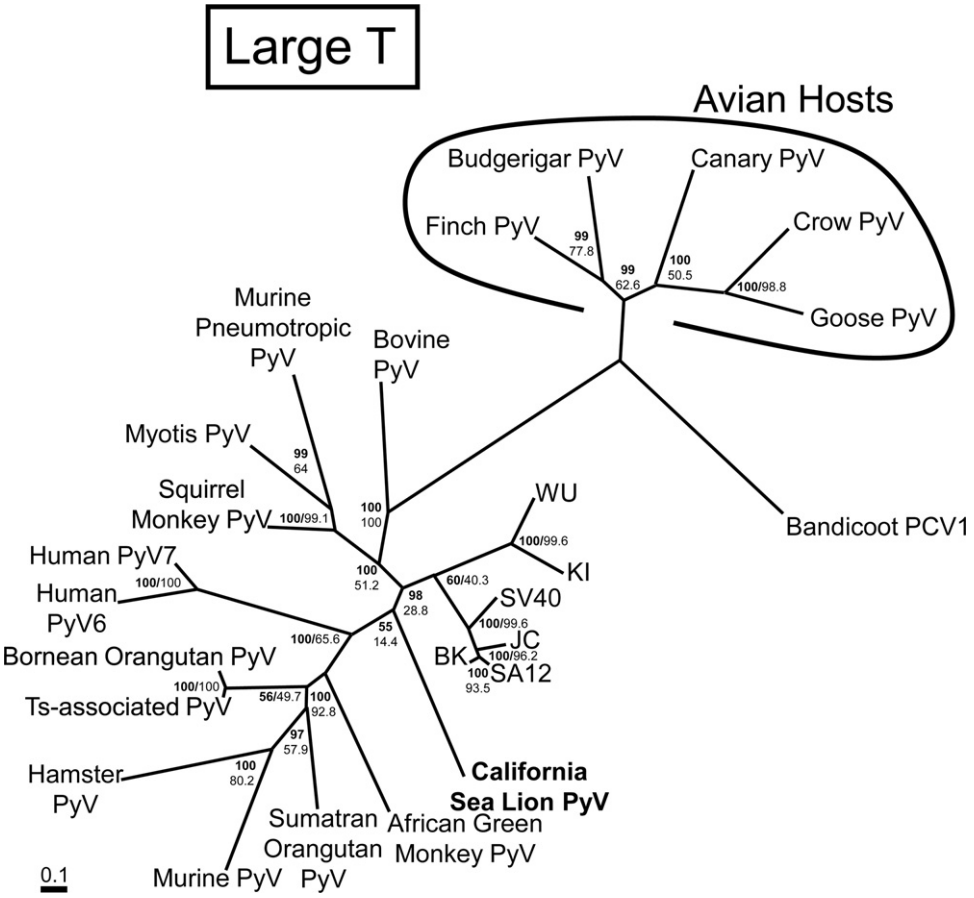

Fig. 6. Bayesian phylogenetic tree of predicted 511–703 amino acid polyomaviral large T second exon sequences based on MAFFT alignment. Bayesian posterior probabilities of clusters as percentages are in bold, and ML bootstrap values for clusters based on 200 re-samplings are given to the right. Bandicoot papillomatosis carcinomatosis virus 1 (GenBank accession number NC010107) was designated as the outgroup. California sea lion polyomavirus 1 is bolded. Bracket shows avian PyV clade. Sequences retrieved from GenBank are as given in the legend for Fig. 2. Merkel cell polyomavirus was not included due to lack of homologous sequence.

was positive with 78 copies, urine had 26 copies, cervix had 4 copies, proximal vagina had 8 copies, and vaginal tumor had 17 copies. Formalin-fixed paraffin-embedded lymph node was also positive with 74 copies present. Frozen urinary bladder and formalin-fixed paraffin-embedded kidney and intestine with lymphoma were negative.

From the additional animals, nine of 43 kidney samples from stranded animals (21%) were positive, and the one kidney examined from the managed population was negative. One of 35 urine samples from stranded animals (3%) was positive, and the one urine sample examined from the managed population was negative. One of six tongue samples from stranded animals (17%) was positive. All buffy coat samples examined from 26 animals in the managed population were negative. In total, polyomavirus infection was found in 13 of 54 (24%) of stranded animals examined. All four additional urinary bladder samples examined were negative, as were the six additional liver samples, six spleen samples, six skin samples, five lymph nodes, four lung samples, four brain samples, three tracheal samples, two esophagus samples, and single samples from mammary gland, vagina, muscle, pericardial fluid, and oral mucosa.

Of the 34 samples found by qPCR to have less than 25 copies detected, 24 were not confirmed by nested PCR and were considered negative. No differences from the reference sequence were seen in any of the 10 positive sequences. Samples confirmed as positive averaged 14.0 predicted copies, whereas those that were rejected averaged 4.6 predicted copies.

4. Discussion

This novel CSLPyV is the first PyV found in the Carnivora, and only the third member of the family found in the Laurasiatheria. Two possible explanations for this include greater distribution of PyVs in Euarchontoglires and lack of screening of the Laurasiatheria. One plausible explanation for a monophyletic laurasiatherian/squirrel monkey PyV/murine pneumotropic virus clade is that this clade evolved in laurasiatherian hosts, with species jumps at some point into squirrel monkeys and mice. Given the monophyly of SqMPyV, MPtV, and Myotis PyV in analyses of every gene, it is plausible that SqMPyV and MPtV are the result of host switches of bat PyVs. The greater pathogenicity of MPtV in mice as compared to Murine PyV may also be suggestive of a shorter host–pathogen relationship.

Lack of support for a laurasiatherian/SqMPyV/MPtV clade in the early region may be due to signal loss or to different evolutionary histories of early/late regions resultant from recombination. While we did not identify recombination sites in our analysis, this may be due to paucity of available taxa. There is evidence of intraspecies recombination of JC virus, where recombination of the early region of one strain and late region of another has been reported (Hatwell and Sharp, 2000). Previous examples of more extreme differences seen between the early and late regions are the bandicoot papillomatosis/carcinomatosis viruses, which have polyomavirus-like early regions and papillomavirus-like late regions (Woolford et al., 2007). In agreement with Krumbholz et al.

(2009), we chose to examine genes separately because of concerns about potential recombination, as has also been shown in the biologically similar papillomaviruses (Shah et al., 2010).

It is often stated that polyomaviruses have codiverged with their hosts, due to a suspected narrow host range and congruence of polyomavirus phylogenies with those of their hosts (Soeda et al., 1980; Shadan and Villarreal, 1993). However, a more recent analysis found limited incongruencies, including failure of rodent and primate PyV to segregate (Pérez-Losada et al., 2006). Another recent analysis of JC virus found that it was not codivergent with human populations and that JC virus evolutionary rates were much more rapid than would be expected with codivergence (Shackelton et al., 2006b). A more recent analysis looking at greater numbers of species did not find support for codivergence (Krumbholz et al., 2009).

The lack of knowledge of polyomaviruses of diverse hosts is particularly troubling for codivergence studies. Host taxa/virus congruence on shorter branches with lack of congruence at deeper branchings may be more consistent with preferential host switching than host/virus codivergence (Jackson and Charleston, 2004). The small genome size of polyomaviruses places limitations on phylogenetic resolution, and the best way to improve this is through including further taxa in analyses. The availability of a more complete representation of existing species for comparison results in greater phylogenetic resolution (Flynn et al., 2005; Stefanovic et al., 2004). Significant errors can occur in phylogenetic analyses due to incomplete taxa sampling, even if very large sequence length is assessed (Lunter, 2007). Previous host/polyomavirus analyses have found segregation between mammal and avian polyomaviruses; our analysis of the small t gene, which includes bandicoot PCV1, fails to find monophyly of the avian polyomaviruses.

We chose to examine amino acid alignments because of concerns regarding non-lineage factors on viral nucleotide composition bias outweighing the true phylogenetic signal. The polyomaviruses are divergent to the point that the NCCR and agnoproteins cannot be reliably aligned, and this indicates that the phylogenetic signal from synonymous sites is likely to be significantly weakened by homoplasy. While it has been shown that nucleotide alignments may be moderately more informative than amino acid alignments when looking at vertebrate genes (Townsend et al., 2008), the small DNA viruses have been shown to have a large bias against CpG dinucleotides (Shackelton et al., 2006a), and it appears that events such as host switches may cause differential biases in different lineages. In the genus *Atadenovirus*, squamate reptiles appear to be the endemic hosts. These viruses appear to have jumped into birds and mammals in at least two separate events, and in both cases, host jumps were associated with a large AT bias (Wellehan et al., 2004). Experimental cross-species transmission of a feline lentivirus was shown to have a major impact on nucleotide bias (Poss et al., 2006). Host nucleotide composition and host switches also appear to have a significant impact on astrovirus composition (van Hemert et al., 2007).

In our amino acid alignments, the carboxy-terminal end of the predicted CSLPyV1 VP1 protein extends 97 amino acids beyond the next longest polyomavirus VP1 protein, from Merkel cell polyomavirus. It extends 134 and 136 amino acids beyond the end of the two polyomavirus VP1 proteins that have had their structures determined, SV40 virus and murine PyV, respectively. In SV40, the best-studied polyomavirus structure, the 49 carboxy-terminal amino acids of VP1 extend from the main portion of the protein on the internal aspect of the capsid, linking to other VP1 pentamer subunits (Stehle et al., 1996).

The putative agnovirus protein, at 50 amino acids, is shorter than any other agnoprotein with the exception of the putative Myotis PyV agnoprotein, which is 30 a.a. (Misra et al., 2009). However, the position in the genome and basic nature are consistent with that of an agnoprotein. Further studies are needed to determine whether this is expressed and functional.

The presence of only two large T binding sites in the NCCR of CSLPyV1 is very unusual. The core element, an area of dyad symmetry normally containing at least three pentamer T antigen recognition sites in either orientation, together with an adjacent poly-A tract, is generally considered the minimum essential region for DNA replication (White et al., 2009). No other known polyomavirus has less than three clustered large T antigen binding sites at the origin of replication. Additionally, there is usually an additional cluster of T antigen recognition sites in the NCCR that was absent in CSLPyV1. In studies with murine polyomavirus, the presence of only a single T antigen recognition site in this additional cluster was associated with weaker association and greater dissociation (Bondeson et al., 1998). One possibility is that CSLPyV1 large T antigen may bind to other sites in addition to GRGGC. However, no significant differences were identified in the region of large T homologous to the DNA binding domain of SV40 (data not shown) (Meinke et al., 2011). The conservation of the 5′ end of the NCCR between CSLPyV1, SqMPyV, and Myotis PyV suggests that this sequence may be functionally important. Future work on NCCR functionality in CSLPyV will require a successful culture system.

It should be noted that our qPCR values are for copies detected, which may potentially differ from actual copy numbers present. We were unable to cultivate virus (data not shown), and hence were unable to spike control samples directly with virus. We used dilutions of known copy numbers of CSLPyV1 DNA as a standard curve. This is of special concern for urine samples; although consistent 18S rRNA amplification was seen in all other samples, it was variable in urine samples. The presence of PCR inhibitors or nucleases in a sample may result in falsely low readings. This caveat should not affect comparison of the same tissue between animals, but caution should be used to avoid overinterpretation when comparing different tissues. Urine does not appear to be an optimal sample for the qPCR protocol described here. Kidney appears to be a reasonable sample for testing, and tongue, liver, lymph node, and esophagus merit further investigation as diagnostic samples. It was mildly surprising, given the apparent endotheliotropism of this virus, that no virus was detected in spleen samples.

No CSLPyV1 was detected in the 26 buffy coats tested. This may be due to lack of viral tropism for this site, or due to the fact that buffy coats tested were from clinically healthy animals from a managed collection and not from stranded animals. Polyomavirus viremia may be seen following reactivation in stressed/immunosuppressed animals (Ziedina et al., 2009), and stranded animals may be more likely to be viremic than clinically normal animals. The infection rate may also differ in the managed population. None of the samples from managed animals were found to be positive. Only two animals from the managed collection had samples surveyed beyond buffy coats, limiting comparisons.

When comparing CSLPyV1 sequences from different samples, no differences were seen in the partial VP1 sequences from 11 samples, partial VP2 sequences from 4 samples, or NCCR from 4 samples. There were two variable nucleotide sites in the shared large T/small t region in the 4 samples examined, and two additional nucleotide sites that were altered in additional carboxy-terminal portions of the small t antigen of the 3 samples examined. Of the variable sites identified, 3 of 4 variations resulted in predicted coding changes. One possible explanation is that positive selection is present at these sites. Positively selected sites have been identified in the small t antigen of Merkel cell PyV and KI PyV (Babakir-Mina et al., 2009, 2010). The region of VP1 examined was not homologous with VP1 regions containing neutralizing epitopes

in SV40 (Murata et al., 2008), and positive selection is more likely at sites of immune recognition.

In conclusion, CSLPyV1 is the first reported polyomavirus of the Carnivora. Phylogenetic analysis found that, at least in the late region, this virus forms a clade with the other known polyomaviruses using laurasiatherian hosts. The VP1 protein and the NCCR of this virus are unusual and merit further study. The qPCR assay developed here can be of use for further surveillance of this virus, and kidney appears to be one reasonable option for testing. Further studies are needed to determine the clinical significance of this virus to populations.

Acknowledgements

This work was funded by Office of Naval Research, Grants Nos. N00014-06-1-0250 and N00014-09-1-0252 to H. Nollens and J. Wellehan, and N66001-08-D-0070 to P. Yochem. The authors would like to thank Liz Wheeler (The Marine Mammal Center), Erica Nilson (SeaWorld San Diego), and Kevin Carlin (U.S. Navy Marine Mammal Program) for assistance with sample collection and Dr. Refugio Robles, Dr. Pam Yochem and Jennifer Burchell from the San Diego Hubbs-SeaWorld Research Institute for laboratory assistance and coordination.

Appendix A. Supplementary data

Supplementary data associated with this article can be found, in the online version, at doi:10.1016/j.meegid.2011.03.010.

References

Altschul, S.F., Madden, T.L., Schäffer, A.A., Zhang, J., Zhang, Z., Miller, W., Lipman, D.J., 1997. Gapped BLAST and PSI-BLAST: a new generation of protein database search programs. Nucleic Acids Res. 25, 3389–3402.

Arroube, A.S., Halami, M.Y., Johne, R., Dorrestein, G.M., 2009. Mortality due to polyomavirus infection in two nightjars (*Caprimulgus europaeus*). J. Avian Med. Surg. 23, 136–140.

Babakir-Mina, M., Ciccozzi, M., Lo Presti, A., Greco, F., Perno, C.F., Ciotti, M., 2010. Identification of Merkel cell polyomavirus in the lower respiratory tract of Italian patients. J. Med. Virol. 82, 505–509.

Babakir-Mina, M., Ciccozzi, M., Bonifacio, D., Bergallo, M., Costa, C., Cavallo, R., Di Bonito, L., Perno, C.F., Ciotti, M., 2009. Identification of the novel KI and WU polyomaviruses in human tonsils. J. Clin. Virol. 46, 75–79.

Bondeson, K., Rönn, O., Magnusson, G., 1998. DNA binding of polyomavirus large T-antigen: kinetics of interactions with different types of binding sites. FEBS Lett. 423, 307–313.

Colegrove, K., Wellehan, J.F.X., Rivera, R., Moore, P.F., Gulland, F.M.D., Lowenstine, L.J., Nordhausen, R.W., Nollens, H.H., 2010. Polyomavirus infection in a free-ranging California sea lion (*Zalophus californianus*). J. Vet. Diagn. Invest. 22, 628–632.

Dimmic, M.W., Rest, J.S., Mindell, D.P., Goldstein, R.A., 2002. rtREV: an amino acid substitution matrix for inference of retrovirus and reverse transcriptase phylogeny. J. Mol. Evol. 55, 65–73.

Dougherty, R.M., 1976. Induction of tumors in Syrian hamsters by a human renal papovavirus, RF strain. J. Natl. Cancer Inst. 57, 395–400.

Felsenstein, J., 1985. Confidence limits on phylogenies: an approach using the bootstrap. Evolution 39, 783–791.

Felsenstein, J., 1989. PHYLIP-Phylogeny inference package. Cladistics 5, 164–166.

Flynn, J.J., Finarelli, J.A., Zehr, S., Hsu, J., Nedbal, M.A., 2005. Molecular phylogeny of the Carnivora (mammalia): assessing the impact of increased sampling on resolving enigmatic relationships. Syst. Biol. 54, 317–337.

Giardi, A.J., Sweet, B.H., Slotnick, V.B., Hilleman, M.R., 1962. Development of tumors in hamsters inoculated in the neonatal period with vacuolating virus, SV-40. Proc. Soc. Exp. Biol. Med. 109, 649–660.

Hatwell, J.N., Sharp, P.M., 2000. Evolution of human polyomavirus JC. J. Gen. Virol. 81, 1191–1200.

Henikoff, S., Henikoff, J.G., 1992. Amino acid substitution matrices from protein blocks. Proc. Natl. Acad. Sci. U.S.A. 89, 10915–10919.

Imperiale, M.J., Major, E.O., 2007. Polyomaviridae. In: Knipe, D.M., Howley, P.M. (Eds.), Field's Virology, 5th ed., vol. 2. Lippincott Williams and Wilkins, Philadelphia, PA, pp. 2263–2298.

Jackson, A.P., Charleston, M.A., 2004. A cophylogenetic perspective of RNA-virus evolution. Mol. Biol. Evol. 21, 45–57.

Jiang, M., Abend, J.R., Johnson, S.F., Imperiale, M.J., 2009. The role of polyomaviruses in human disease. Virology 384, 266–273.

Johne, R., Müller, H., 2007. Polyomaviruses of birds: etiologic agents of inflammatory disease in a tumor virus family. J. Virol. 81, 11554–11559.

Johne, R., Paul, G., Enderlein, D., Stahl, T., Grund, C., Müller, H., 2007. Avian polyomavirus mutants with deletions in the VP4-encoding region show deficiencies in capsid assembly and virus release, and have reduced infectivity in chicken. J. Gen. Virol. 88, 823–830.

Jones, D.T., Taylor, W.R., Thornton, J.M., 1992. The rapid generation of mutation data matrices from protein sequences. Comput. Appl. Biosci. 8, 275–282.

Katoh, K., Toh, H., 2008. Recent developments in the MAFFT multiple sequence alignment program. Brief Bioinform. 9, 286–298.

Khalili, K., White, M.K., Sawa, H., Nagashima, K., Safak, M., 2005. The agnoprotein of polyomaviruses: a multifunctional auxiliary protein. J. Cell. Physiol. 204, 1–7.

Kidney, B.A., Haines, D.M., Ellis, J.A., Burnham, M., Jackson, M.L., 2001. Evaluation of formalin-fixed paraffin-embedded tissues from vaccine site-associated sarcomas of cats for polyomavirus DNA and antigen. Am. J. Vet. Res. 62, 828–832.

Kosiol, C., Goldman, N., 2005. Different versions of the Dayhoff rate matrix. Mol. Biol. Evol. 22, 193–199.

Krumbholz, A., Bininda-Emonds, O.R., Wutzler, P., Zell, R., 2009. Phylogenetics, evolution, and medical importance of polyomaviruses. Infect. Genet. Evol. 9, 784–799.

London, W.T., Houff, S.A., Madden, D.L., Fuccillo, D.A., Gravell, M., Wallen, W.C., Palmer, A.E., Sever, J.L., Padgett, B.L., Walker, D.L., ZuRhein, G.M., Ohashi, T., 1978. Brain tumors in owl monkeys inoculated with a human polyomavirus (JC virus). Science 201, 1246–1249.

London, W.T., Houff, S.A., McKeever, P.E., Wallen, W.C., Sever, J.L., Padgett, B.L., Walker, D.L., 1983. Viral-induced astrocytomas in squirrel monkeys. Prog. Clin. Biol. Res. 105, 227–237.

Lunter, G., 2007. Dog as an outgroup to human and mouse. PLoS Comput. Biol. 3, e74.

Martin, D.P., Williamson, C., Posada, D., 2005. RDP2: recombination detection and analysis from sequence alignments. Bioinformatics 21, 260–262.

Meinke, G., Phelan, P.J., Fradet-Turcotte, A., Bohm, A., Archambault, J., Bullock, P.A., 2011. Structure-based analysis of the interaction between the simian virus 40 T-antigen origin binding domain and single-stranded DNA. J. Virol. 85, 818–827.

Mes, T.H., van Doornum, G.J., Schutten, M., 2010. Population genetic tests suggest that the epidemiologies of JCV and BKV are strikingly different. Infect. Genet. Evol. 10, 397–403.

Misra, V., Dumonceaux, T., Dubois, J., Willis, C., Nadin-Davis, S., Severini, A., Wandeler, A., Lindsay, R., Artsob, H., 2009. Detection of polyoma and corona viruses in bats of Canada. J. Gen. Virol. 90, 2015–2022.

Murata, H., Teferedegne, B., Sheng, L., Lewis Jr., A.M., Peden, K., 2008. Identification of a neutralization epitope in the VP1 capsid protein of SV40. Virology 381, 116–122.

Murphy, W.J., Eizirik, E., O'Brien, S.J., Madsen, O., Scally, M., Douady, C.J., Teeling, E., Ryder, O.A., Stanhope, M.J., de Jong, W.W., Springer, M.S., 2001. Resolution of the early placental mammal radiation using Bayesian phylogenetics. Science 294, 2348–2351.

Pérez-Losada, M., Christensen, R.G., McClellan, D.A., Adams, B.J., Viscidi, R.P., Demma, J.C., Crandall, K.A., 2006. Comparing phylogenetic codivergence between polyomaviruses and their hosts. J. Virol. 80 (June (12)), 5663–5669 2006.

Pinkerton, M.E., Wellehan, J.F.X., Johnson, A.J., Childress, A.L., Fitzgerald, S.D., Kinsel, M.J., 2008. Columbid herpesvirus-1 in two Cooper's hawks (*Accipiter cooperii*) with fatal inclusion body disease. J. Wildl. Dis. 44, 622–628.

Poss, M., Ross, H.A., Painter, S.L., Holley, D.C., Terwee, J.A., Vandewoude, S., Rodrigo, A., 2006. Feline lentivirus evolution in cross-species infection reveals extensive G-to-A mutation and selection on key residues in the viral polymerase. J. Virol. 80, 2728–2737.

Ronquist, F., Huelsenbeck, J.P., 2003. MRBAYES 3: Bayesian phylogenetic inference under mixed models. Bioinformatics 19, 1572–1574.

Sastre-Garau, X., Peter, M., Avril, M.F., Laude, H., Couturier, J., Rozenberg, F., Almeida, A., Boitier, F., Carlotti, A., Couturaud, B., Dupin, N., 2009. Merkel cell carcinoma of the skin: pathological and molecular evidence for a causative role of MCV in oncogenesis. J. Pathol. 218, 48–56.

Shackelton, L.A., Parrish, C.R., Holmes, E.C., 2006a. Evolutionary basis of codon usage and nucleotide composition bias in vertebrate DNA viruses. J. Mol. Evol. 62, 551–563.

Shackelton, L.A., Rambaut, A., Pybus, O.G., Holmes, E.C., 2006b. JC virus evolution and its association with human populations. J. Virol. 80, 9928–9933.

Shadan, F.F., Villarreal, L.P., 1993. Coevolution of persistently infecting small DNA viruses and their hosts linked to host-interactive regulatory domains. Proc. Natl. Acad. Sci. U.S.A. 90, 4117–4121.

Shah, S.D., Doorbar, J., Goldstein, R.A., 2010. Analysis of host-parasite incongruence in papillomavirus evolution using importance sampling. Mol. Biol. Evol. 27, 1301–1314.

Soeda, E., Maruyama, T., Arrand, J.R., Griffin, B.E., 1980. Host-dependent evolution of three papova viruses. Nature 285, 165–167.

Sroller, V., Vilchez, R.A., Stewart, A.R., Wong, C., Butel, J.S., 2008. Influence of the viral regulatory region on tumor induction by simian virus 40 in hamsters. J. Virol. 82, 871–879.

Stefanovic, S., Rice, D.W., Palmer, J.D., 2004. Long branch attraction, taxon sampling, and the earliest angiosperms: *Amborella* or monocots? BMC Evol. Biol. 4 (1), 35.

Stehle, T., Gamblin, S.J., Yan, Y., Harrison, S.C., 1996. The structure of simian virus 40 refined at 3.1 Å resolution. Structure 4, 165–182.

Streicker, D.G., Turmelle, A.S., Vonhof, M.J., Kuzmin, I.V., McKracken, G.F., Rupprecht, C.E., 2010. Host phylogeny constrains cross-species emergence and establishment of rabies virus. Science 329, 676–679.

Townsend, J.P., López-Giráldez, F., Friedman, R., 2008. The phylogenetic informativeness of nucleotide and amino acid sequences for reconstructing the vertebrate tree. J. Mol. Evol. 67, 437–447.

van Hemert, F.J., Berkhout, B., Lukashov, V.V., 2007. Host-related nucleotide composition and codon usage as driving forces in the recent evolution of the Astroviridae. Virology 361, 447–454.

Veerassamy, S., Smith, A., Tillier, E.R., 2003. A transition probability model for amino acid substitutions from blocks. J. Comput. Biol. 10, 997–1010.

Verschoor, E.J., Groenewoud, M.J., Fagrouch, Z., Kewalapat, A., van Gessel, S., Kik, M.J., Heeney, J.L., 2008. Molecular characterization of the first polyomavirus from a New World primate: squirrel monkey polyomavirus. J. Gen. Virol. 89, 130–137.

Walker, D.L., Padgett, B.L., ZuRhein, G.M., Albert, A.E., Marsh, R.F., 1973. Human papovavirus (JC): induction of brain tumors in hamsters. Science 100, 674–676.

Wellehan, J.F.X., Johnson, A.J., Harrach, B., Benkö, M., Pessier, A.P., Johnson, C.M., Garner, M.M., Childress, A., Jacobson, E.R., 2004. Detection and analysis of six lizard adenoviruses by consensus primer PCR provides further evidence of a reptilian origin for the atadenoviruses. J. Virol. 78, 13366–13369.

Whelan, S., Goldman, N., 2001. A general empirical model of protein evolution derived from multiple protein families using a maximum-likelihood approach. Mol. Biol. Evol. 18, 691–699.

White, M.K., Safak, M., Khalili, K., 2009. Regulation of gene expression in primate polyomaviruses. J. Virol. 83, 10846–10856.

Woolford, L., Rector, A., Van Ranst, M., Ducki, A., Bennett, M.D., Nicholls, P.K., Warren, K.S., Swan, R.A., Wilcox, G.E., O'Hara, A.J., 2007. A novel virus detected in papillomas and carcinomas of the endangered western barred bandicoot (*Perameles bougainville*) exhibits genomic features of both the Papillomaviridae and Polyomaviridae. J. Virol. 81, 13280–13290.

Ziedina, I., Folkmane, I., Chapenko, S., Murovska, M., Sultanova, A., Jushinskis, J., Rozental, R., 2009. Reactivation of BK virus in the early period after kidney transplantation. Transplant. Proc. 41, 766–768.